

# CHEMISTRY

## A European Journal

A Journal of



### Accepted Article

**Title:** Functional Conjugated Polymers for CO<sub>2</sub> Reduction Using Visible Light

**Authors:** Can Yang, Wei Huang, Lucas Caire da Silva, Kai A. I. Zhang, and Xinchun Wang

This manuscript has been accepted after peer review and appears as an Accepted Article online prior to editing, proofing, and formal publication of the final Version of Record (VoR). This work is currently citable by using the Digital Object Identifier (DOI) given below. The VoR will be published online in Early View as soon as possible and may be different to this Accepted Article as a result of editing. Readers should obtain the VoR from the journal website shown below when it is published to ensure accuracy of information. The authors are responsible for the content of this Accepted Article.

**To be cited as:** *Chem. Eur. J.* 10.1002/chem.201804496

**Link to VoR:** <http://dx.doi.org/10.1002/chem.201804496>

Supported by  
**ACES**

WILEY-VCH

# Functional Conjugated Polymers for CO<sub>2</sub> Reduction Using Visible Light

Can Yang,<sup>[a]</sup> Wei Huang,<sup>[b]</sup> Lucas Caire da Silva,<sup>[b]</sup> Kai A. I. Zhang,<sup>\*,[b]</sup> and Xinchen Wang<sup>\*,[a]</sup>

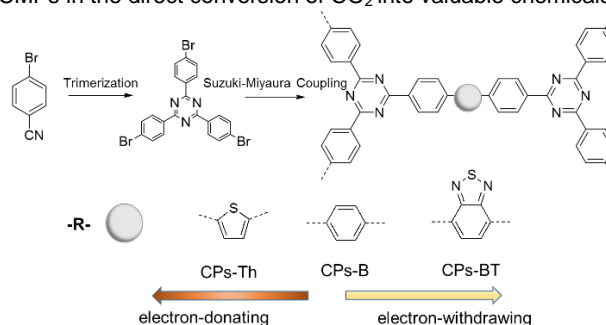
**Abstract:** The reduction of CO<sub>2</sub> with visible light is a highly sustainable method for producing valuable chemicals. The functional design of organic conjugated semiconductors with more chemical variety than that of inorganic semiconductors has emerged as a method for achieving carbon photofixation chemistry. Here, we report the molecular engineering of triazine-based conjugated microporous polymers to capture, activate and reduce CO<sub>2</sub> to CO with visible light. The optical band gap of the CMPs is engineered by varying the organic electron-withdrawing (benzothiadiazole) and electron-donating units (thiophene) on the skeleton of the triazine rings while creating organic Donor-Acceptor junctions to promote the charge separation. This engineering also provides control of the texture, surface functionality and redox potentials of CMPs for achieving the light-induced conversion of CO<sub>2</sub> to CO ambient conditions.

The conversion of CO<sub>2</sub> by light into valuable C1/C2 chemicals provides a sustainable solution to addressing environmental and energy issues.<sup>[1-5]</sup> However, the activation of the stable carbon-oxygen bond in a CO<sub>2</sub> molecule to achieve the subsequent reduction has proven highly challenging. Enormous research efforts have been devoted to the development of catalytic systems for direct CO<sub>2</sub> conversion.<sup>[6-9]</sup> Inspired by photosystem I (PS I) in natural photosynthesis, which directly converts CO<sub>2</sub> into hydrocarbons by using sunlight at room temperature and ambient pressure, two different reduction pathways, i.e., electroreduction or photoreduction, have been developed to activate the carbon-oxygen bond of CO<sub>2</sub>. For example, atomic metal,<sup>[10]</sup> metal oxides,<sup>[11]</sup> metal chalcogenides,<sup>[12,13]</sup> metal-organic complexes<sup>[14]</sup> and heteroatom-doped carbon materials<sup>[15,16]</sup> have been used to catalytically induce the electroreduction of CO<sub>2</sub>. To achieve the direct conversion of CO<sub>2</sub> by photoreduction, transition metal complexes<sup>[17]</sup> or semiconductors<sup>[18,19]</sup> and metal-decorated zeolites<sup>[20,21]</sup> have been investigated; however, conjugated organic semiconductors have been rarely studied during the last 50 years.

Recently, conjugated polymer systems have gained considerable attention as visible-light-active and metal-free photocatalysts due to their easy ability to influence various properties by varying their semiconductor characteristics.<sup>[22,23]</sup> One of the most promising examples is binary graphitic carbon nitride (g-CN),<sup>[24]</sup> which has been utilised in CO<sub>2</sub> photoreduction

because of its basic sites, tunable structure and N-rich surface functional groups. For example, Wang *et al.* reported that g-CN copolymerized from urea and organic monomers was used to promote the photochemical conversion of CO<sub>2</sub>.<sup>[25]</sup> Very recently, Maeda *et al.* designed a novel catalytic system for CO<sub>2</sub> reduction with a turnover number of 2000 and a selectivity of 98% based on Ag-modified g-CN with Ru<sup>II</sup> binuclear complexes.<sup>[26]</sup>

Conjugated polymers (CPs), another emerging class of heterogeneous and metal-free photocatalysts, are of particular interest due to their highly tunable electronic and optical properties, morphology and porosity on account of the large synthetic variety in their structure formation.<sup>[27,28]</sup> In particular, the semiconductor redox potentials of CPs can be precisely modified via electron donor or electron acceptor combinations, which in principle also create organic dyadic structure to facilitate charge separation. Recent research has demonstrated the use of CMPs in a variety of organic photoredox reactions.<sup>[29-32]</sup> Cooper *et al.* reported the use of CMPs with an optical band gap ranging from 2.95 eV to 1.94 eV for photocatalytic hydrogen production via water splitting.<sup>[33]</sup> We recently reported a series of benzothiadiazole-containing CMPs as heterogeneous photocatalysts for hydrogen production.<sup>[34]</sup> Other conjugated systems containing benzene and spirobifluorene or triazine-based polymer networks<sup>[35-37]</sup> have been developed for utilization in photocatalytic hydrogen production. Owing to their strong CO<sub>2</sub>-philicity,<sup>[38-41]</sup> the incorporation of triazine functional groups in polymeric networks should facilitate CO<sub>2</sub> photoreduction process. What's more, photocatalytic CO<sub>2</sub> reduction using CPs-based semiconductors has barely been reported. It is therefore time to examine the feasibility of applying CMPs in the direct conversion of CO<sub>2</sub> into valuable chemicals.



**Scheme 1.** Illustrated design and synthesis pathway of three triazine-based polymers with different molecular structures for photocatalytic CO<sub>2</sub> reduction.

Here, we have studied the utilization of CPs for the reduction of CO<sub>2</sub> and investigated the impact of the structure on their catalytic efficiency. In this study, three CPs were designed and obtained via coupling 2,4,6-tris(4-bromophenyl)-1,3,5-triazine (TBPT-Br) with 1,4-phenylenediboronic acid (B), 2,5-thiophenediboronic acid (Th) and 2,1,3-benzothiadiazole-4,7-bis(boronic acid pinacol ester) (BT) as electron donor and acceptor building blocks. This coupling was done using palladium-

[a] Dr. C. Yang, Prof. X. Wang  
State Key Laboratory of Photocatalysis on Energy and Environment,  
College of Chemistry  
Fuzhou University, Fuzhou 350116, P. R. China  
E-mail: [xcwang@fzu.edu.cn](mailto:xcwang@fzu.edu.cn)

[b] Dr. W. Huang, Dr. L. C. Silva, Dr. K. A. I. Zhang,  
Max Planck Institute for Polymer Research  
Ackermannweg 10, 55128 Mainz, Germany  
E-mail: [kai.zhang@mpip-mainz.mpg.de](mailto:kai.zhang@mpip-mainz.mpg.de)

Supporting information for this article is given via a link at the end of the document.

catalysed Suzuki cross-coupling polycondensation reaction to form the corresponding conjugated polymer networks CPs-B, CPs-Th and CPs-BT, respectively. The structures of the three CPs are illustrated in Figure 1. The detailed synthetic procedures and characterization data are described in the Supporting Information (SI). By the incorporation of different electron donor or acceptor units, the efficiency of photocatalytic CO<sub>2</sub> reduction into CO could be enhanced, giving CO formation rates of up to 18.2  $\mu\text{mol h}^{-1}$ . A selectivity of 81.6% was achieved with a maximal apparent quantum yield (AQY) of 1.75% at 405 nm in a water/acetonitrile/triethanolamine reaction medium. As a side product, the formation of H<sub>2</sub> gas was also identified with a hydrogen evolution rate (HER) of 4.1  $\mu\text{mol h}^{-1}$ .

The triazine-based CPs were obtained as powders, which were insoluble in all common organic and aqueous solvents tested. Interestingly, scanning electron microscopy (SEM) and transmission electron microscopy (TEM) both revealed a hollow nanotubular morphology. The CPs-BT hollow nanotubes had an average length of approximately 25  $\mu\text{m}$  with an inner diameter of approximately 135 nm and a wall thickness of approximately 60 nm (Fig. 1a, b). The elemental mapping images (Fig. 1c) and EDX (Fig. S1) of CPs-BT clearly illustrated that it contained C, N and S. The morphology of polymer CPs-B and CPs-Th was also nanotubes but distinguished from CPs-BT in the size (Fig. S2). This observation of the nanotubular morphology of the CPs was similar to that of previous reports on CPs containing triazine units.<sup>[42]</sup> The exact formation mechanism is unclear. However, we believe that it might be caused by the low solubility of the triazine monomer (TBPT-Br) and the assembly effect, which resulted in a dimethylformamide (DMF)/water mixture during the polymerization process.

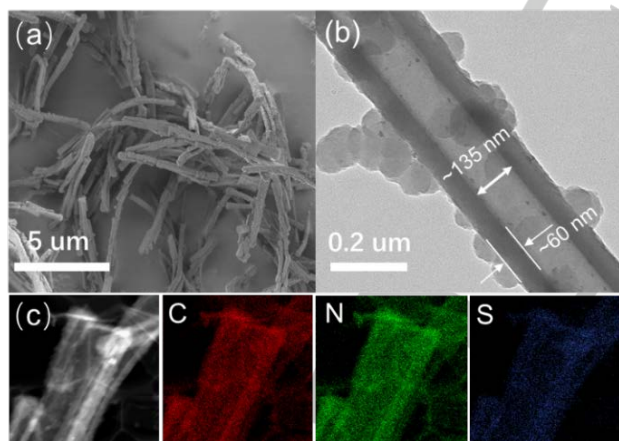


**Figure 1.** Characteristics of CPs-BT Nanotube Morphology. (a) The SEM and (b) TEM images and (c) Element Mapping of C, N and S.

The Fourier transform infrared (FT-IR) spectra of the three CPs contained two characteristic and intense peaks at 1505 and 1360  $\text{cm}^{-1}$  in Fig. 2a, which could be ascribed to the aromatic C-N stretching and breathing modes of the triazine unit. The signals at 1572 and 1603  $\text{cm}^{-1}$  could be assigned to the skeletal vibration of the typical aromatic rings in the polymers. Solid-state <sup>13</sup>C cross-polarization magic-angle-spinning (CP-MAS) NMR spectroscopy unambiguously confirmed the presence of triazine,

as seen in the similar signals at 170 ppm for the sp<sup>2</sup> carbons of three polymers (Fig. 2b).<sup>30, 34</sup> The chemical shifts at 127 ppm and 134 ppm could be attributed to the phenyl carbons. The specific peak for CPs-BT at 152.7 ppm can be assigned to the carbon adjacent to the nitrogen atom in the BT units. The chemical structures of another two CPs were also demonstrated by NMR spectrum (Fig. S4). Thermogravimetric analysis (TGA) revealed high thermal stabilities for the three polymers up to approximately 400 °C (Fig. S5). The powder X-ray diffraction (PXRD) pattern shown in Fig. S6 revealed the amorphous character of the three CPs. In addition, the porosity of the CPs nanotubes was measured by N<sub>2</sub> gas sorption at 77 K, and the Brunauer-Emmett-Teller (BET) surface areas were 409, 52 and 37 m<sup>2</sup> g<sup>-1</sup> for CPs-B, CPs-Th and CPs-BT, respectively (shown in Fig. S7). In addition to the micropores, pronounced pore size distributions ranging between 2.3 and 5 nm were observed for CPs-Th and CPs-BT. This result could possibly be caused by the low cross-linking degree of both CPs, which also explains their low BET surface areas.

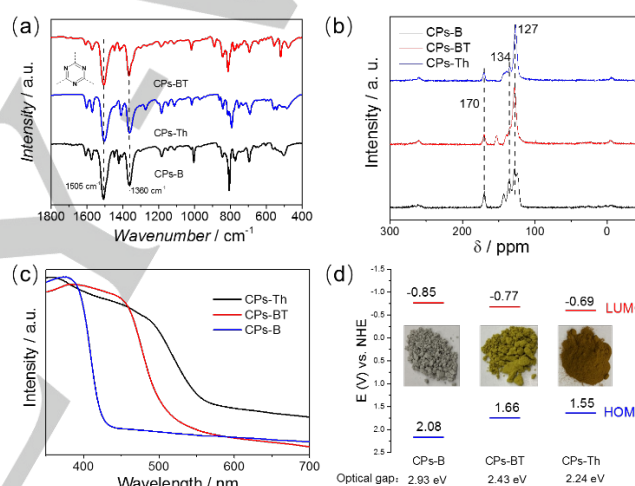


**Figure 2.** Characteristics of Chemical Structure and Optical Properties. (a) FT-IR spectra of three CP materials; (b) Solid state <sup>13</sup>C CP/MAS spectra of three CPs; (c) UV/vis Diffuse Reflectance Spectra of CMPs and their corresponding photograph. (d) Cyclic voltammetry (CV) plots and HOMO/LUMO energy levels for CPs-B, CPs-BT, and CPs-Th.

The UV/vis diffuse reflectance spectra (DRS) of the polymers were displayed in Fig. 2c. The polymers exhibited different optical properties. CPs-B showed an absorption range of up to 423 nm with an optical band gap of 2.93 eV. CPs-Th, which contained thiophene as electron donor units, showed an absorption range of up to 510 nm and an optical band gap of 2.43 eV. With the incorporation of electron-withdrawing units, *i.e.*, benzothiadiazole, into the CPs backbone, an absorption range of up to 554 nm was observed, resulting in an optical band gap of 2.24 eV. Cyclic voltammetry (CV) measurements were conducted (Figure S6) to enable precise study of the highest occupied molecular orbital (HOMO) and the lowest unoccupied molecular orbital (LUMO) of the polymers. The HOMO levels were observed at 1.81, 1.42 and 1.31 V, and the LUMO levels were observed at -1.12, -1.01 and -0.93 V for CPs-B, CPs-BT and CPs-Th, respectively (Figs. 3d and S8), which is enough for the reduction of CO<sub>2</sub>. Furthermore, we examined the (photo)-

electrochemical properties of the polymers by electrochemical impedance spectroscopy and photocurrent measurements (see Fig. S9). The minimum Nyquist radius and an enhanced photocurrent generated on CPs-BT suggested an improved charge separation and transfer in photocatalysis.

The activities of the CPs in CO<sub>2</sub> reduction was investigated in a water/acetonitrile/TEOA reaction medium. TEOA acted as an extra sacrificial electron donor. CoCl<sub>2</sub> and dipyrindyl were added into the catalytic system as an electron-mediating co-catalyst to enhance charge separation and promote the transfer kinetics and interfacial interactions. The results were listed in Table 1. Gas chromatography mass spectrometry analysis (GC-MS) with isotope labelling in an extra control experiment under <sup>12</sup>CO<sub>2</sub> and <sup>13</sup>CO<sub>2</sub> atmospheres was conducted to confirm that the CO originated from CO<sub>2</sub> reduction (Fig. S10). Among the three CPs, CPs-BT appeared to be the best photocatalyst, with a CO formation rate of 18.2 μmol h<sup>-1</sup> (In Table 1, Entries 1-3) and a high selectivity of 81.6%. Interestingly, the formation of H<sub>2</sub> gas with an evolution rate of 4.1 μmol h<sup>-1</sup> was also observed. The highest photocatalytic efficiency of CPs-BT could result from the incorporation of electron-withdrawing BT units into the triazine poly-network. This in turn could enhance charge separation and further improve light-induced electron transfer reactions.

**Table 1.** Photocatalytic CO<sub>2</sub> reduction into CO by the CMPs.

Entry	Cat.	CO/μmol·h <sup>-1</sup>	H <sub>2</sub> /μmol·h <sup>-1</sup>	Sel.co <sup>[b]</sup> / %
1	CPs-B	4	2	66.7
2	CPs-Th	10	3	76.9
3	CPs-BT	18.2	4.1	81.6
4 <sup>[c]</sup>	CPs-BT	n. d.	n. d.	/
5	/	n. d.	n. d.	/
6 <sup>[d]</sup>	CPs-BT	n. d.	0.18	/
7 <sup>[e]</sup>	CPs-BT	0.35	2.51	12.2
8 <sup>[f]</sup>	CPs-BT	n. d.	1.04	/

[a] Standard reaction conditions: CMP (15 mg), CoCl<sub>2</sub> (1 μmol), dipyrindyl (5 μmol), solvent (5 mL, acetonitrile/water = 4:1), TEOA (1 mL), CO<sub>2</sub> (1 atm.), white light (λ ≥ 420 nm), 30 °C 1 h. [b] Sel.CO% = n(CO)/n(CO+H<sub>2</sub>) × 100%. [c] in dark. [d] Without TEOA. [e] Without CoCl<sub>2</sub>/dipyrindyl. [f] Replace CO<sub>2</sub> with Ar gas. n. d. = not detectable.

To explain the mechanics of light-induced CO<sub>2</sub> reduction, we conducted a series of control experiments using CPs-BT as a photocatalyst. There was no detectable formation of CO and H<sub>2</sub> when the experiments were performed in the absence of the CPs or light (Entries 4-5). Without using TEOA, no CO was determined however, a small amount of H<sub>2</sub> (Entry 6) was detected. In the absence of Co<sup>2+</sup>, decreases in the CO and H<sub>2</sub> formation rates were determined (Entry 7). This demonstrates the positive role of Co<sup>2+</sup> as an electron mediator, which can enhance the catalytic efficiency of CO<sub>2</sub> photoreduction. When the reaction mixture was exposed to an Ar atmosphere instead of CO<sub>2</sub>, only H<sub>2</sub> formation was observed, demonstrating the activity of the polymer photocatalyst for H<sub>2</sub> evolution (Entry 8).

We then turned our attention to studies of the solvent effect to reveal the reaction mechanism (Figure S9). Different solvents, such as acetonitrile (MeCN), N,N-dimethylformamide (DMF),

1,4-dioxane (DOA), tetrahydrofuran (THF), dichloromethane (DCM) and trifluorotoluene (TFT), were first tested without using water as a co-solvent. A clear tendency was observed showing that strong, polar and nitrogen- or oxygen-containing solvents could enhance the reduction of CO<sub>2</sub> to CO. Among the solvents, the highest CO formation rate (8.7 μmol h<sup>-1</sup>) was observed in DMF. This indicates a possible enhanced solubilizing effect of CO<sub>2</sub> resulting from the Lewis acid-base interactions in those solvents (Fig. S11a). Significantly, by adding water into the solvents, a general increase in the CO formation rate was achieved, with a 1:4 ratio of MeCN/H<sub>2</sub>O being the best solvent combination (Fig. S11b and Table S1). The addition of water as a co-solvent ought to have a combined solubilizing and further reducing effect for CO<sub>2</sub>. This effect was achieved through the formation of reactive protons [H] via water splitting by the polymer photocatalyst, as demonstrated before.<sup>[23]</sup>

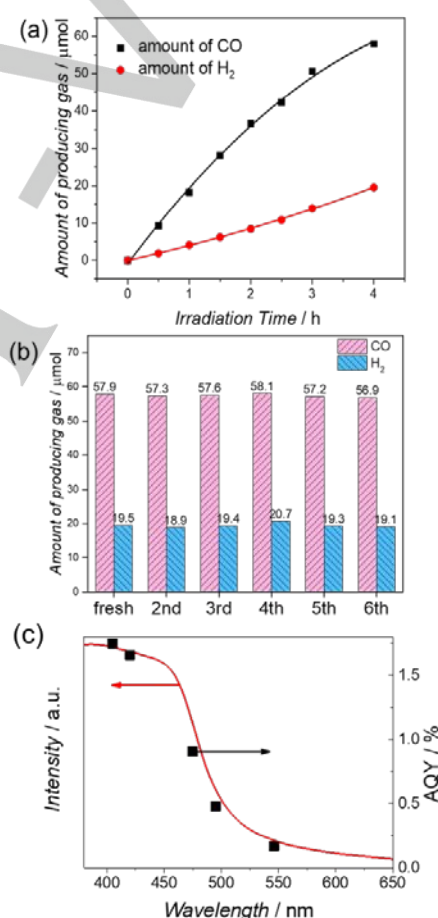


**Figure 3.** Conversion of CO<sub>2</sub> to CO by photocatalyst CPs-BT. (a) Time dependence of CO and H<sub>2</sub> generation rate using CPs-BT (15 mg) as a photocatalyst under visible light irradiation (λ > 420 nm) for 4 h. (b) Stability and Reusability tests for CO<sub>2</sub> reduction. (c) Wavelength dependence of AQY for the H<sub>2</sub> and CO production at 405, 420, 470, 490 and 546 nm, respectively.

The time dependence of the CO<sub>2</sub> reduction rate using CPs-BT as a photocatalyst was shown in Fig. 3a. After a reaction period of 4 h, 60 μmol of CO gas was obtained. Repeated experiments showed that similar amounts of CO were produced



after six additional cycles, demonstrating the high stability and reusability of CPs-BT as a photocatalyst (Fig. 3b). During the recyclability experiments, more than 400  $\mu\text{mol}$  of CO gas was generated, corresponding to a catalytic turnover number of  $\sim 20$  for CPs-BT and  $\sim 400$  for the cobalt co-catalyst. No apparent change was observed in both FT-IR (Fig. S12) and DRS (Fig. S13) spectrum of CPs-BT to demonstrate the excellently stable chemical structure in conjugated networks. The wavelength dependence of the apparent quantum yield of CO and  $\text{H}_2$  production was illustrated for CPs-BT in Figure 3c, with the highest AQY of ca. 1.75% at 405 nm. In addition, some reported modified polymeric photocatalysts with similar chemical structures (such as carbon nitride and BCN systems) for  $\text{CO}_2$  reduction were listed in Table S2, the triazine-based CPs polymer especially CPs-BT possessed a superior photocatalytic activity with high selectivity.

In summary, we designed triazine-based CPs to be used as emerging photocatalysts for visible-light-promoted reduction of  $\text{CO}_2$  to CO. By varying the organic electron-withdrawing and electron-donating units in the triazine-based polymer backbone, the charge separation kinetics and catalytic reaction kinetics can be promoted to enable the stable photoconversion of  $\text{CO}_2$  to CO under visible light irradiation, giving an AQY of 1.75% at 405 nm. By studying the reaction mechanism, we were able to observe the enhancing effect of the strong polar and nitrogen- or oxygen-containing solvents on the efficiency. This work demonstrates a correlation between the structure of conjugated polymer photocatalysts to their photocatalytic performance in  $\text{CO}_2$  reduction, which could open a new avenue for carbon photofixation by using soft organic conjugated polymers with the ability to easily modify their chemical composition, electronic structure and surface functionality.

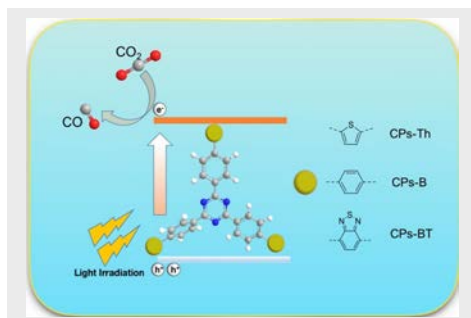
## Acknowledgements

This work was financially supported by the National Key Technologies R & D Program of China (2018YFA0209301), the National Natural Science Foundation of China (21802022, 21425309, 21761132002, and 21861130353) and the 111 Project (D16008). C. Y. thanks the support of Guest PhD Program from Graduate School of Material Science in Mainz and PPP project (201801940015). W. H. acknowledges the scholarship of the China Scholarship Council (CSC). K. A. I. Z. acknowledges the Max Planck Society for financial support.

**Keywords:** organic semiconductor • conjugated polymers • triazine-based polymers •  $\text{CO}_2$  reduction

- [1] Y. Izumi, *Coord. Chem. Rev.* **2013**, *257*, 171-186.
- [2] N. S. Lewis; D. G. Nocera, *Proc. Natl. Acad. Sci.* **2006**, *103*, 15729-15735.
- [3] A. Listorti, J. Durrant, J. Barber, *Nat Mater* **2009**, *8*, 929-930.
- [4] W. Tu, Y. Zhou, Z. Zou, *Adv. Mater.* **2014**, *26*, 4607-4626.
- [5] O. K. Varghese, M. Paulose, T. J. Latempa, C. A. Grimes, *Nano Lett.* **2009**, *9*, 731.
- [6] C. Song, *Catal. Today* **2006**, *115*, 2-32.
- [7] L. N. He, J. Q. Wang, J. L. Wang, *Pure Appl. Chem.* **2009**, *81*, 2069-2080.
- [8] M. Shi, Y. Shen, *Curr. Org. Chem.* **2003**, *7*, 737-745.
- [9] Y. Yang, S. Ajmal, X. Zheng, L. Zhang, *Sustainable Energy Fuels*, **2018**, *2*, 510-537.
- [10] S. Gao, Y. Lin, X. Jiao, Y. Sun, Q. Luo, W. Zhang, D. Li, J. Yang, Y. Xie, *Nature* **2016**, *529*, 68-71.
- [11] Y. Chen, M. W. Kanan, *J. Am. Chem. Soc.* **2012**, *134*, 1986-1989.
- [12] X. Sun, Q. Zhu, X. Kang, H. Liu, Q. Qian, Z. Zhang, B. Han, *Angew. Chem., Int. Ed.* **2016**, *55*, 6771-6775.
- [13] A. Manzi, T. Simon, C. Sonleitner, M. Döblinger, R. Wyrwich, O. Stern, J. K. Stolarczyk, J. Feldmann, *J. Am. Chem. Soc.* **2015**, *137*, 14007-14010.
- [14] Z. Weng, J. Jiang, Y. Wu, Z. Wu, X. Guo, K. L. Materna, W. Liu, V. S. Batista, G. W. Brudvig, H. Wang, *J. Am. Chem. Soc.* **2016**, *138*, 8076-8079.
- [15] T. Liu, S. Ali, Z. Lian, B. Li, D. S. Su, *J. Mater. Chem. A* **2017**, *5*, 21596-21603.
- [16] X. Duan, J. Xu, Z. Wei, J. Ma, S. Guo, S. Wang, H. Liu, S. Dou, *Adv. Mater.* **2017**, *29*, 1701784.
- [17] H. Rao, L. C. Schmidt, J. Bonin, M. Robert, *Nature* **2017**, *548*, 74-77.
- [18] S. N. Habisreutinger, L. Schmidt-Mende, J. K. Stolarczyk, *Angew. Chem. Int. Ed.* **2013**, *52*, 7372-7408.
- [19] Y. Chen, G. Jia, Y. Hu, G. Fan, Y. H. Tsang, Z. Li, Z. Zou, *Sustainable Energy Fuels* **2017**, *1*, 1875-1898.
- [20] S. Wang, X. Wang, *Angew. Chem. Int. Ed.*, **2016**, *55*, 2308-2320.
- [21] W. Lin, H. Frei, *J. Am. Chem. Soc.* **2005**, *127*, 1610-1611.
- [22] A. G. Slater, A. I. Cooper, *Science* **2015**, *348*, 8075.
- [23] H. Xu, J. Gao, D. Jiang, *Nat. Chem.* **2015**, *7*, 905-912.
- [24] X. Wang, K. Maeda, A. Thomas, K. Takanabe, G. Xin, J. M. Carlsson, K. Domen, M. Antonietti, *Nat. Mater.* **2009**, *8*, 76-80.
- [25] J. Qin, S. Wang, H. Ren, Y. Hou, X. Wang, *Appl. Catal. B: Environ.* **2015**, *179*, 1-8.
- [26] R. Kuriki, M. Yamamoto, K. Higuchi, Y. Yamamoto, M. Akatsuka, D. Lu, S. Yagi, T. Yoshida, O. Ishitani, K. Maeda, *Angew. Chem. Int. Ed.* **2017**, *56*, 4867-4871.
- [27] M. Rose, *ChemCatChem* **2014**, *6*, 1166-1182.
- [28] J. Jiang, F. Su, A. Trewin, C. D. Wood, N. L. Campbell, H. Niu, C. Dickinson, A. Y. Ganin, M. J. Rosseinsky, Y. Z. Khimyak, A. I. Cooper, *Angew. Chem. Int. Ed.* **2007**, *46*, 8574-8578.
- [29] K. Zhang, D. Kopetzki, P. H. Seeberger, M. Antonietti, F. Vilela, *Angew. Chem. Int. Ed.* **2013**, *52*, 1432-1436.
- [30] Z. J. Wang, S. Ghasimi, K. Landfester, K. A. I. Zhang, *Chem. Commun.* **2014**, *50*, 8177-80.
- [31] S. Ghasimi, S. Prescher, Z. J. Wang, K. Landfester, J. Yuan, K. A. I. Zhang, *Angew. Chem. Int. Ed.* **2016**, *54*, 14549-14553.
- [32] W. Huang, B. C. Ma, H. Lu, R. Li, L. Wang, K. Landfester, K. A. I. Zhang, *ACS Catal.* **2017**, *7*, 5438-5442.
- [33] R. S. Sprick, J.-X. Jiang, B. Bonillo, S. Ren, T. Ratvijitvech, P. Guiglion, M. A. Zwijnenburg, D. J. Adams, A. I. Cooper, *J. Am. Chem. Soc.* **2015**, *137*, 3265-3270.
- [34] C. Yang, B. C. Ma, L. Zhang, S. Lin, S. Ghasimi, K. Landfester, K. A. I. Zhang, X. Wang, *Angew. Chem. Int. Ed.* **2016**, *55*, 9202-9206.
- [35] L. Stegbauer, K. Schwinghammer, B. V. Lotsch, *Chem. Sci.* **2014**, *5*, 2789-2793.
- [36] K. Wang, L. Yang, X. Wang, L. Guo, G. Cheng, C. Zhang, S. Jin, B. Tan, A. I. Cooper, *Angew. Chem. Int. Ed.* **2017**, *56*, 14149-14153.
- [37] K. Schwinghammer, S. Hug, M. B. Mesch, J. Senker, Lotsch, B. V., *Energy Environ. Sci.* **2015**, *8*, 3345-3353.
- [38] P. Kuhn, M. Antonietti, A. Thomas, *Angew. Chem. Int. Ed.* **2008**, *47*, 3450-3453.
- [39] X. Zhu, C. Tian, S. Mahurin, S. Chai, C. Wang, S. Brown, G. Veith, H. Luo, H. Liu, S. Dai, *J. Am. Chem. Soc.* **2012**, *134*, 10478-10484.
- [40] S. Ren, M. Bojdis, R. Dawson, A. Laybourn, Y. Khimyak, D. Adams, A. I. Cooper, *Adv. Mater.* **2012**, *24*, 2357-2361.
- [41] X. Zhu, S. Mahurin, S. An, C. Do-Thanh, C. Tian, Y. Li, L. Gill, E. Hagaman, Z. Bian, J. Zhou, J. Hu, H. Liu, S. Dai, *Chem. Commun.* **2014**, *50*, 7933-7936.
- [42] M. Wang, L. Guo, D. Cao, *Sci. China Chem.* **2017**, *60*, 1090-1097.

The optical band gap of the triazine-based conjugated polymers were engineered by varying the organic electron-withdrawing and electron-donating units on the skeleton of the triazine rings while controlling of the texture, surface functionality and redox potentials for achieving the conversion of CO<sub>2</sub> to CO.



C. Yang, W. Huang, L. C. Silva, K. A. I. Zhang,\* and X. Wang\*

Page No. – Page No.

Functional Conjugated Polymers for CO<sub>2</sub> Reduction Using Visible Light